

Branched Hamiltonians and Supersymmetry

T L Curtright[§] and C K Zachos[‡]

[§]Department of Physics, University of Miami, Coral Gables, FL 33124-8046, USA
curtright@miami.edu

[‡]High Energy Physics Division, Argonne National Laboratory, Argonne, IL 60439-4815, USA
zachos@anl.gov

Abstract

Some examples of branched Hamiltonians are explored both classically and in the context of quantum mechanics, as recently advocated by Shapere and Wilczek. These are in fact cases of switchback potentials, albeit in momentum space, as previously analyzed for quasi-Hamiltonian chaotic dynamical systems in a classical setting, and as encountered in analogous renormalization group flows for quantum theories which exhibit RG cycles. A basic two-worlds model, with a pair of Hamiltonian branches related by supersymmetry, is considered in detail.

1 Introduction

Multi-valued Hamiltonians have appeared in at least two contexts. Most recently, they have resulted from Legendre transforming Lagrangians whose velocity dependence is not convex [1, 2], which invariably leads to a Riemann surface phase-space structure, with multiply-branched Hamiltonians, and to interesting topological issues [3, 4]. Previously, they have arisen in the continuous interpolation of discrete time dynamical systems, particularly those systems that exhibited chaotic behavior, where they could be incorporated in a canonical “quasi-Hamiltonian” formalism [5, 6, 7, 8].

Moreover, by analogy with quasi-Hamiltonian systems, renormalization group flows that exhibit cycles have also been shown to be governed by multi-valued β functions [9, 10].

We consider here several simple Lagrangian models that lead to double-valued Hamiltonian systems, to illuminate “two-worlds theory.” We begin with an example where the velocity dependence of L is given by a gaussian. This example illustrates many generic features of branched Hamiltonians, in addition to its more specific peculiarities. In particular, as a quantum system the gaussian model is not amenable to solution in closed form, so we turn to a different class of models where analytic results can be obtained. One of the models in this class is tailored so as to have a pair of Hamiltonians that comprise a supersymmetric quantum mechanical system [11]. This facilitates obtaining analytic results as well as numerical study of this special model.

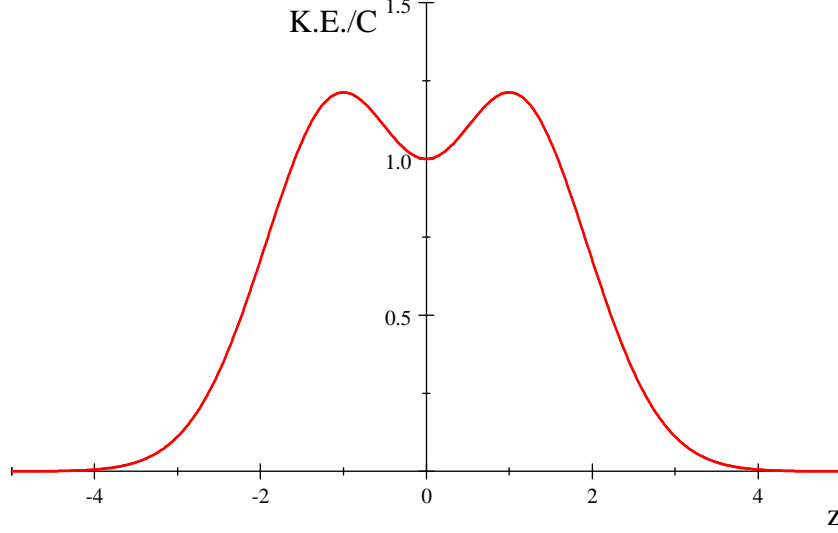
2 A gaussian model with momentum switchbacks

For an interesting example, consider a non-convex v -dependent gaussian Lagrangian:

$$L(x, v) = C \left(1 - \exp \left(-\frac{1}{2C} m v^2 \right) \right) - V(x) , \quad (1)$$

$$p(v) = \frac{\partial L}{\partial v} = m v \exp \left(-\frac{1}{2C} m v^2 \right) . \quad (2)$$

Most of what can be said about this model can be stated at the classical level. L is a union of three convex functions defined on the three v intervals $(-\infty, -\sqrt{C/m}]$, $[-\sqrt{C/m}, \sqrt{C/m}]$, and $[\sqrt{C/m}, \infty)$. The width parameter C sets the energy scale. When plotted versus v , the kinetic energy of the model has the classic shape of a *fedora* hat profile.



Kinetic energy, $(L + V) / C = \left(1 + \frac{mv^2}{C}\right) e^{-\frac{1}{2} \frac{mv^2}{C}}$, versus $z \equiv v\sqrt{m/C}$, for the gaussian model.

For this model, v and p always have the same sign, and clearly $-\infty \leq v \leq +\infty$. However, due to the gaussian suppression in v , the momentum p is confined to a *finite* interval, as given by the maximum and minimum of (2), namely, $p(v)|_{v=\pm\sqrt{C/m}} = \pm\sqrt{mC/e}$.

Moreover, there are two values for H at every value of $p \in (-\sqrt{mC/e}, \sqrt{mC/e})$. To see this double-valued H , we invert (2) to obtain

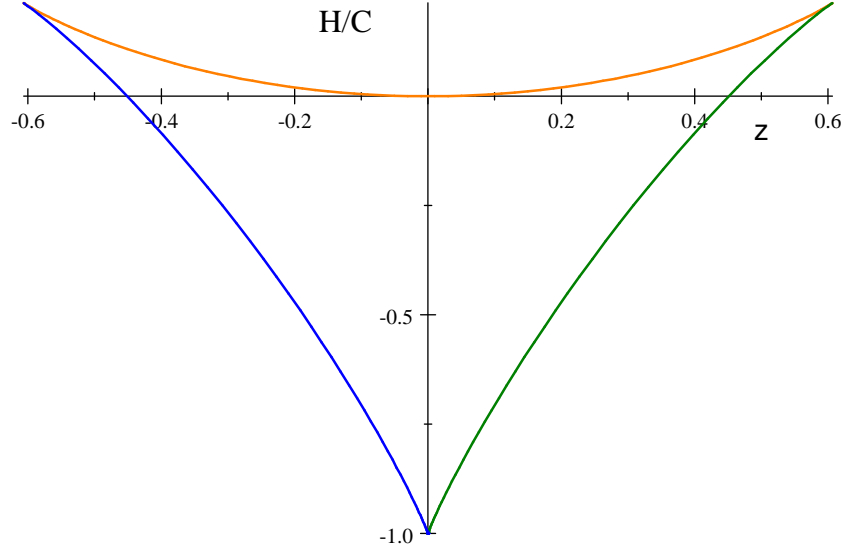
$$v(p) = \pm \sqrt{-\frac{C}{m} \text{LambertW}\left(-\frac{p^2}{mC}\right)}, \quad (3)$$

where both real branches of the negatively-valued Lambert function, for negative argument, are allowed. Thus the Hamiltonian, $H(x, p) = p v(p) - L(x, v(p))$, as a function of position and momentum, is

$$\begin{aligned} H(x, p) &= \sqrt{\frac{Cp^2}{m}} \left(\pm \sqrt{-\text{LambertW}\left(-\frac{p^2}{mC}\right)} \pm \frac{1}{\sqrt{-\text{LambertW}\left(-\frac{p^2}{mC}\right)}} \right) - C + V(x) \\ &= V(x) + \frac{1}{2m} p^2 + \frac{1}{8Cm^2} p^4 + \frac{5}{48m^3C^2} p^6 + O(p^8), \end{aligned} \quad (4)$$

where the low momentum expansion is valid near $p = 0$ for the upper, principal branch of the Lambert function.

Now, since there are *two* real branches for both the square-root function and the Lambert function, we might expect four values for H at any given momentum. However, the square-root and LambertW branches are always correlated, as is evident upon considering the $(p(v), H(x, p(v)))$ curve in parametric form on the (p, H) plane, using v as the parameter, so that the gaussian model's Hamiltonian is only double-valued for all $p \in (-\sqrt{mC/e}, \sqrt{mC/e})$. This is shown in the following Figure for $V(x) = 0$. Note the Hamiltonian curve closes, as a function of p , with three cusps.



The real branches of H/C versus $z \equiv p/\sqrt{mC} \in [-1/\sqrt{e}, 1/\sqrt{e}] \approx [-0.61, 0.61]$.

While only double-valued, H is clearly the union of *three* convex functions, defined on three overlapping momentum intervals: H_- , H_0 , and H_+ for $p \in [-\sqrt{mC/e}, 0]$, $[-\sqrt{mC/e}, \sqrt{mC/e}]$, and $[0, \sqrt{mC/e}]$, as displayed in the Figure in blue, orange, and green, respectively.

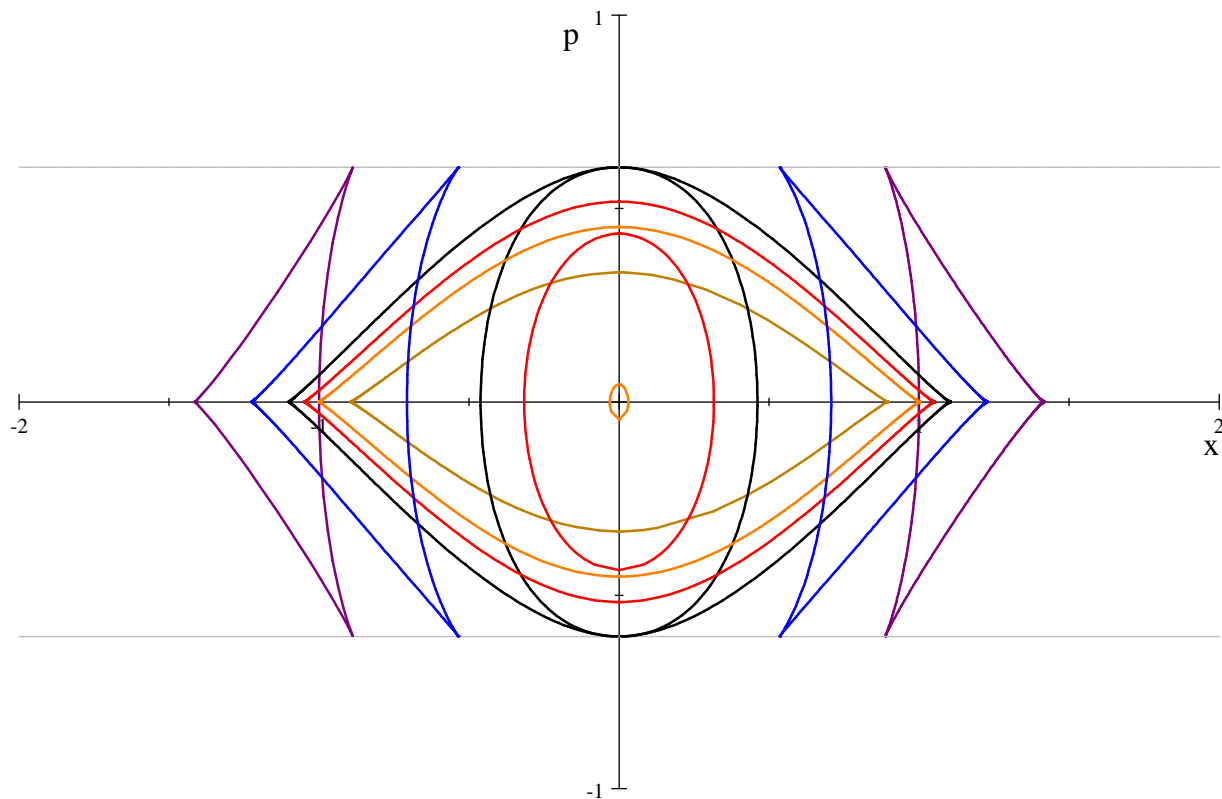
Classical trajectories for this model, given a specific choice for $V(x)$, evince the switchback potential phenomena discussed at length in [6], only here in momentum rather than position space.

For instance, selecting the harmonic potential, $V(x) = C + \frac{1}{2}m\omega^2x^2$, it is straightforward to plot trajectory curves in terms of either (x, v) or (x, p) . Some explicit (x, p) phase space trajectories for various fixed energies are plotted below (for $\frac{1}{2}m\omega^2 = 1 = C$). More information is available online, where trajectories are also shown on the (x, v) configuration surface (a cylinder, actually).

When moving on a trajectory governed by one branch of H , a classical particle will encounter one of the Hamiltonian cusps in finite time, in general, and then bounce (switch) to be governed by another branch of H . Because of this switching, trajectories may intersect and cross in the Figure. This cannot happen for a system governed by a single-valued Hamiltonian, as is well-known, but it is allowed when different Hamiltonian branches are governing the motion for the different curves that cross. A system governed by a multi-valued Hamiltonian usually does exhibit this novel feature. We have called such trajectories “quasi-Hamiltonian” flows in our earlier work [6].

The unified 3-fold structure of H brings to mind some previous theories exhibiting triality [12], along with supersymmetry. However, to our knowledge the gaussian model above shows no compelling signs of supersymmetry. Still, it would be quite interesting to find a simple, three-Hamiltonian, single-particle quantum system, based on a single unifying Lagrangian, that could be partitioned into pairs of supersymmetric Hamiltonians, with state-linking operators of a type familiar from supersymmetric quantum mechanics.

In the following Sections, we will analyze a different model with a double-valued Hamiltonian that *does* exhibit supersymmetry. But first some preliminaries. The gaussian model does not readily admit analytic, closed form results when quantized, even with so simple a potential as $V(x) = C + \frac{1}{2}m\omega^2x^2$, so we turn to a class of models where exact quantum results can be more easily obtained.



Gaussian model phase space trajectories for $E = 2/\sqrt{e} \approx 1.21$, $E = 3/2$, & $E = 2$ are shown in black, blue, & purple, respectively, and also for $E = 0.800$, 1.001 , & 1.100 , in sienna, orange, & red, respectively. The black curves constitute a separatrix. The outer, black, cusped curve is approached from within by trajectories whose E is increased from 0 to $2/\sqrt{e}$, while the inner, black oval is approached not only from without by the cusped, triangular trajectories, as E is decreased to $2/\sqrt{e}$, but also from within by bounded, closed oval orbits, as E is increased from 1 to $2/\sqrt{e}$.

3 A class of double-valued Hamiltonians

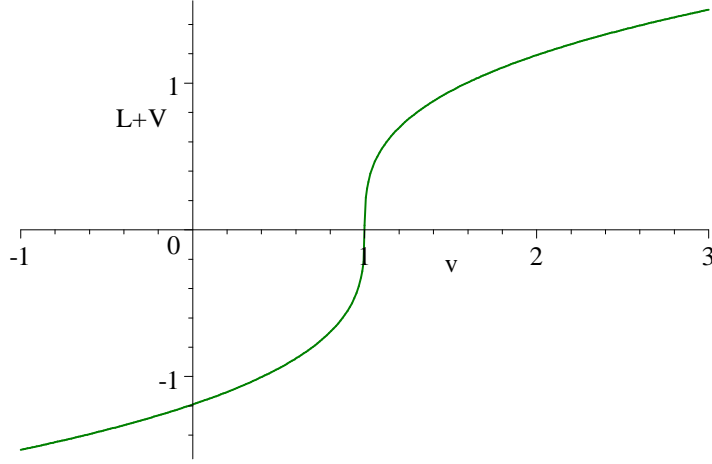
For positive integer k , consider¹

$$L = C(v-1)^{\frac{2k-1}{2k+1}} - V(x) \quad \text{with} \quad C \equiv \frac{2k+1}{2k-1} \left(\frac{1}{4}\right)^{\frac{2}{2k+1}} > 0. \quad (5)$$

For real v we take the $1/(2k+1)$ roots to be real, such that $(v-1)^{\frac{1}{2k+1}} \geq 0$ for $v \geq 1$. By doing this we are in fact taking the real parts of two different branches of the analytic $1/(2k+1)$ roots as a function of complex v . We do this solely to have a real, single-valued Lagrangian function for *all* real v .

So far as we can tell, there is no particularly compelling reason not to draw on more than one branch of an analytic function of v so long as only one branch is encountered at any given real v , or at least that would seem to be true for classical dynamics. We will discuss the consequences this choice for L has for the quantum dynamics in the following, especially for the case $k = 1$.

¹This class of models could be generalized to $L = C(v-c)^{n/m} - V(x)$ for any fixed c & C , and for any odd integer n & odd integer m . There seems to be no real gain or simplification achieved by doing so, except perhaps for the choice $c = 0$.



The $k = 1$ case, $L + V = C(v - 1)^{\frac{1}{3}}$.

For v near zero, we then have $L \approx C \left(-1 + v \frac{2k-1}{2k+1} + v^2 \frac{2k-1}{(2k+1)^2} + O(v^3) \right)$. Of these terms, the first is innocuous, the second would give a boundary contribution to the action and therefore not effect the equations of motion, and the third is the usual v^2 kinetic structure:

$$\begin{aligned}
A &= \int_{t_1}^{t_2} L dt \\
&\approx C \left(t_2 - t_1 + \frac{2k-1}{2k+1} (x(t_2) - x(t_1)) + \frac{2k-1}{(2k+1)^2} \int_{t_1}^{t_2} v^2 dt + \int_{t_1}^{t_2} O(v^3) dt \right) \\
&\quad - \int_{t_1}^{t_2} V(x) dt .
\end{aligned} \tag{6}$$

So this action would yield the usual Newtonian classical equations of motion for small v . On the other hand, for large velocities, the v dependence is more elaborate, leading (for finite, positive integer k) to a non-convex function of velocity, whose curvature $\partial^2 L / \partial v^2$ flips sign at just one point, namely, $v = 1$.

Thus, the function L may be thought of a single *pair* of convex functions judiciously pieced together. The non-convexity of L has the effect of making the kinetic energy, and hence the Hamiltonian, a *double-valued* function of p . For any positive integer k , we find *two* branches for H ,

$$H_{\pm} = p \pm \frac{1}{4k-2} \left(\frac{1}{\sqrt{p}} \right)^{2k-1} + V(x) . \tag{7}$$

This follows from

$$p = \partial L / \partial v = \left(\frac{1}{4} \right)^{\frac{2}{2k+1}} \frac{1}{[(v-1)^2]^{1/2k+1}} , \tag{8}$$

whose inverse $v(p)$ is double-valued,

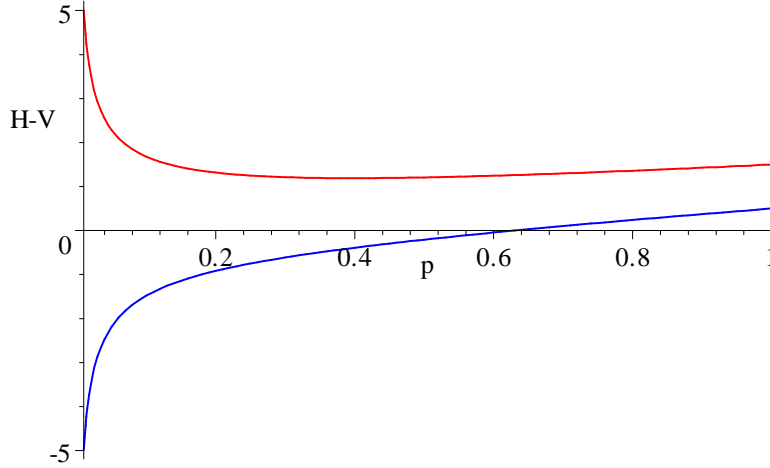
$$v_{\pm}(p) \equiv 1 \mp \frac{1}{4} \left(\frac{1}{\sqrt{p}} \right)^{2k+1} . \tag{9}$$

The pair of Hamiltonians in (7) are then obtained by taking the *Legendre transform* with respect to each of the two v branches,

$$H_{\pm}(x, p) = p v_{\pm}(p) - L , \tag{10}$$

where we have used $L(x, p) = \mp \frac{1}{4} \frac{2k+1}{2k-1} \left(\frac{1}{\sqrt{p}} \right)^{2k-1} - V(x)$ on the $v_{\pm}(p)$ branches.

For $k = 1$, the two kinetic energy branches have the shape shown in the Figure below. Note that, *classically*, p must be non-negative for this model to avoid imaginary $v(p)$. That is to say, the slope $\partial L / \partial v$ is always positive.



$H_{\pm} - V(x)|_{k=1} = p \pm \frac{1}{2\sqrt{p}}$ in red/blue. There is a cusp at $p = \infty$ where both $H_{\pm} \sim p$.

Following the suggestions of Shapere and Wilczek [2], we define the associated *quantum* theory with $p \geq 0$ as a restriction, with various boundary conditions imposed on the wave functions, $\psi(p)$, at $p = 0$, such that there is no probability flow to negative p .

4 A supersymmetric model

We purposefully plotted the $k = 1$ case of (5), and related quantities, in the above Figures. The $k = 1$ case is special when the potential $V(x)$ is harmonic: It is a *supersymmetric* quantum mechanical system when viewed in momentum space. In that case, $C = 3/4^{2/3} \approx 1.19$ and

$$L = C(v-1)^{1/3} - V(x) \xleftrightarrow{\text{Legendre}} H_{\pm} = p \pm \frac{1}{2\sqrt{p}} + V(x), \quad (11)$$

$$V(x) = x^2 \xrightarrow{\text{QM in } p \text{ space}} -\frac{d^2}{dp^2}. \quad (12)$$

4.1 Quantum features

The momentum space pair of QM Hamiltonian operators for this case is therefore expressible in the standard form for a supersymmetric pair,

$$H_{\pm} = -\frac{d^2}{dp^2} + w_0^2(p) \pm w_0'(p) = \left(\frac{d}{dp} \pm w_0(p) \right) \left(-\frac{d}{dp} \pm w_0(p) \right), \quad (13)$$

where $w_0(p) = \sqrt{p}$. This has the interesting feature that the true — square-integrable — ground state of the system is non-vanishing for only one of the branches, namely, H_- .

As an algebraic system, for $p \geq 0$, the two Hamiltonians are related in a familiar fashion by

$$H_- = a^\dagger a, \quad H_+ = aa^\dagger = H_- + [a, a^\dagger] = H_- + 1/\sqrt{p}, \quad (14)$$

$$a \equiv \frac{d}{dp} + \sqrt{p}, \quad a^\dagger \equiv -\frac{d}{dp} + \sqrt{p}, \quad [a, a^\dagger] = \frac{1}{\sqrt{p}}. \quad (15)$$

Both energy spectra are non-negative given either Dirichlet or Neumann boundary conditions at $p = 0$.²

The zero-energy ground state of H_- is given by

$$a\psi_0(p) = 0, \quad \psi_0(p) = N_0 \exp\left(-\frac{2}{3}p^{3/2}\right), \quad N_0 = \frac{6^{1/6}}{\sqrt{\Gamma(\frac{2}{3})}} \approx 1.16. \quad (16)$$

This obeys the boundary condition $\psi'_0(0) = 0 \neq \psi_0(0)$, and is normalized such that $\int_0^\infty |\psi_0(p)|^2 dp = 1$.

On the other hand, the zero-energy state for H_+ , namely, $\phi(x) = \exp\left(+\frac{2}{3}p^{3/2}\right)$, is not admissible, because it has infinite norm.

The higher energy states are degenerate, with $H_\pm \psi^{(\pm)} = E\psi^{(\pm)}$ eigenstates for $E > 0$ mutually related by

$$\psi_E^{(+)} = \frac{1}{\sqrt{E}} a\psi_E^{(-)}, \quad \psi_E^{(-)} = \frac{1}{\sqrt{E}} a^\dagger \psi_E^{(+)}, \quad (17)$$

so as to have equal norms. In particular the first excited state for H_- is degenerate with the lowest energy state for H_+ , with $E_1 = 1.89379$, as determined by numerical analysis.

All this conforms with well-known expectations for general supersymmetric QM. Due to the restriction $p \geq 0$, there is perhaps an interesting wrinkle here, albeit previously encountered for the supersymmetric simple harmonic oscillator (but normally expressed in terms of $\psi(x)$): The degenerate H_\pm eigenfunctions obey different boundary conditions at $p = 0$. If one is Dirichlet, the other is Neumann. This follows from the mutual relations between $\psi_E^{(\pm)}$ and the fact that a and a^\dagger reduce to $\pm d/dp$ when acting on nonsingular functions at $p = 0$. For example, the first H_- excited state and its degenerate H_+ partner eigenstate satisfy $\psi_{E_1}^{(-)}|_{p=0} = 0 = d\psi_{E_1}^{(+)}|_{p=0}$, while for the next excited states, $d\psi_{E_2}^{(-)}|_{p=0} = 0 = \psi_{E_2}^{(+)}|_{p=0}$, etc.

Flipping the boundary conditions actually has a practical benefit due to the $1/\sqrt{p}$ singularity in both H_\pm : It is more straightforward to perform an accurate numerical computation of the energy eigenvalue using the boundary condition $\psi_E(0) = 0 \neq \psi'_E(0)$ than it is using the condition $\psi_E(0) \neq 0 = \psi'_E(0)$. The degeneracy of the eigenfunctions permits one to always choose the $\psi_E(0) = 0$ condition, along with the corresponding H_+ or H_- .

These higher energy states may be thought of as a single nontrivial state defined on a unified covering space — a double covering of the half-line \mathbb{R}_+ by \mathbb{R} — obtained by unfolding the two Hamiltonian branches to obtain a single H [2] globally defined on \mathbb{R} . However, as is clear from the preceding discussion, the true ground state of the system is $\psi_0(p) \cup 0$ on the unfolded space. The latter, somewhat unusual feature is possible because the two Hamiltonians on the half-lines join together in a cusp at $p = \infty$, where ψ_0 and all its derivatives vanish. So too vanish all the higher $\psi_E^{(\pm)}$ and all their derivatives at $p = \infty$.

For this reason, it would be excusable not to have thought of the degenerate eigenstates on the half-line as two branches of a single function. However, the unified two-worlds picture provided by joining them together on a covering real line, with Neumann and Dirichlet boundary conditions at opposite ends, is a

²There is a subtlety here. Strictly, a^\dagger is *not* the adjoint of a . For states subject to Neumann conditions, $\psi|_{p=0} \neq 0 = \psi'|_{p=0}$, there are nonvanishing boundary contributions at $p = 0$: $\int_0^\infty (\psi_2(a^\dagger\psi_1^*) - \psi_1^*(a\psi_2)) dp = \psi_1^*\psi_2|_{p=0}$. Nevertheless, it is still true for ψ satisfying *either* Neumann *or* Dirichlet conditions that $\langle H_- \rangle = \int_0^\infty |a\psi|^2 dp \geq 0$ and $\langle H_+ \rangle = \int_0^\infty |a^\dagger\psi|^2 dp \geq 0$, because for such states, $\psi^*(a\psi)|_{p=0} = 0 = \psi^*(a^\dagger\psi)|_{p=0}$.

more compelling point of view, in our opinion. Perhaps more importantly, this omniscient view of the two-worlds system becomes natural when the common Lagrangian underpinning both H_{\pm} is considered.

Self-adjointness of H and probability flow. For arbitrary superpositions of momentum space wave functions, $\psi = \sum_n c_n \psi_n$, with each of the ψ_n obeying either Dirichlet or Neumann boundary conditions, the Hamiltonians are real but not self-adjoint. While the behavior at $p = \infty$ is sufficiently benign for all normalizable linear combinations of energy eigenfunctions, the behavior at $p = 0$ could be a problem since

$$\int_0^{\infty} ((H_{\pm}\chi^*)\psi - \chi^*(H_{\pm}\psi)) dp = \psi \frac{d}{dp}\chi^* \Big|_{p=0} - \chi^* \frac{d}{dp}\psi \Big|_{p=0}, \quad (18)$$

and this does not necessarily vanish. To avoid this and ensure self-adjointness of H , a superselection rule may be imposed [13]: The Hilbert space may be partitioned into Dirichlet and Neumann solutions, $\mathcal{H} = \mathcal{H}_D \oplus \mathcal{H}_N$, while allowing no mixing of the two. Thus, superpositions of only Dirichlet or only Neumann wave functions are permitted, but linear combinations of both are not.

While restrictive, this rule nevertheless retains the novel double-valued Hamiltonian feature of the model. Both branches of H_{\pm} are operative on each of \mathcal{H}_D and \mathcal{H}_N . Linear combinations of progressively higher energy levels that alternate between H_- and H_+ eigenstates, i.e. $\psi = \sum_n b_n \psi_{E_n}^{(-)} + c_n \psi_{E_{n+1}}^{(+)}$, maintain the self-adjointness of H , while requiring both H_{\pm} for their time evolution.

The same superselection rule guarantees conservation of probability at $p = 0$. Wave packets in either \mathcal{H}_D or \mathcal{H}_N will not transport probability to negative p .

4.2 Classical features

It is also instructive to survey essential features of the classical trajectories for the model. The Euler-Lagrange equations are

$$\frac{dv}{dt} = \frac{9}{C} x \sqrt[3]{(v-1)^5}. \quad (19)$$

where $9/C = 3 \times 4^{2/3} \approx 7.56$. So we immediately see there are *special solutions*: $v = 1$ for any initial x results in $v(t) = 1$ for all t . Therefore, for any $x(0)$,

$$x(t) = x(0) + t. \quad (20)$$

More generally, if $v > 1$ at any time, then it will remain so for all t , the force does not restore, and x will grow with t , faster than exponential in fact. In this case the time it takes for x to go to ∞ is finite. But if $v < 1$ at any time, it will remain so for all t , the force is restoring, and the solution oscillates, albeit nonlinearly.

Classically, energy conservation along a given configuration space trajectory may be expressed as constant E where

$$E(x, v) = x^2 + \frac{C}{3} \frac{3 - 2v}{\sqrt[3]{(v-1)^2}}. \quad (21)$$

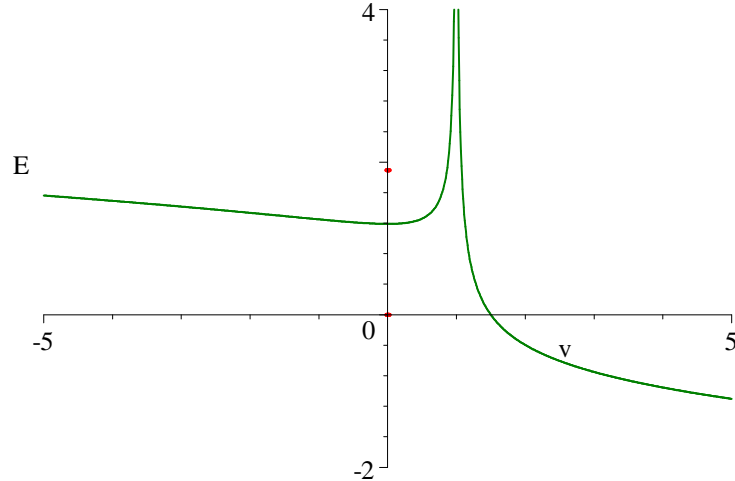
Note that this E is *single-valued* as a function of v , even though $H_{\pm}(x, v) = vp_{\pm}(v) - L(x, v)$ is *double-valued* as a function of v .

How can this be? It is possible just because the two branches of $H_{\pm}(x, v)$ appear on *opposite* sides of $v = 1$, and not for the same value of v . That is to say, it all comes back to our choice for the cube roots on the real line. By taking L real for both $v > 1$ and for $v < 1$, we have in fact used two different branches of the analytic cube root function defined for complex z . However, with our construction, we encounter only one branch of this analytic function, and hence one value of L , at any given real value of v . The story is different for the two Hamiltonians, $H_{\pm}(x, p)$, where we encounter both branches for every $p > 0$.

Upon detailed inspection of constant $E(x, v)$ curves on the (x, v) plane, one finds that, for $E < C$, there are only open trajectories with $v > 1$, and all these escape to $x = \infty$ in finite times, in which case only $H_-(x, p)$ is operative; while for $E \geq C$, on the (x, v) plane there are not only open, unbounded trajectories, for all $v > 1$, as governed again by $H_-(x, p)$, but also closed, bounded trajectories, for all $v < 1$, as governed by $H_+(x, p)$.

Hence for $E \geq C$ classical trajectories exist in which both H_+ and H_- are operative. This should be compared with the existence of admissible wave functions for both H_{\pm} with identical energy eigenvalues $E > C$.

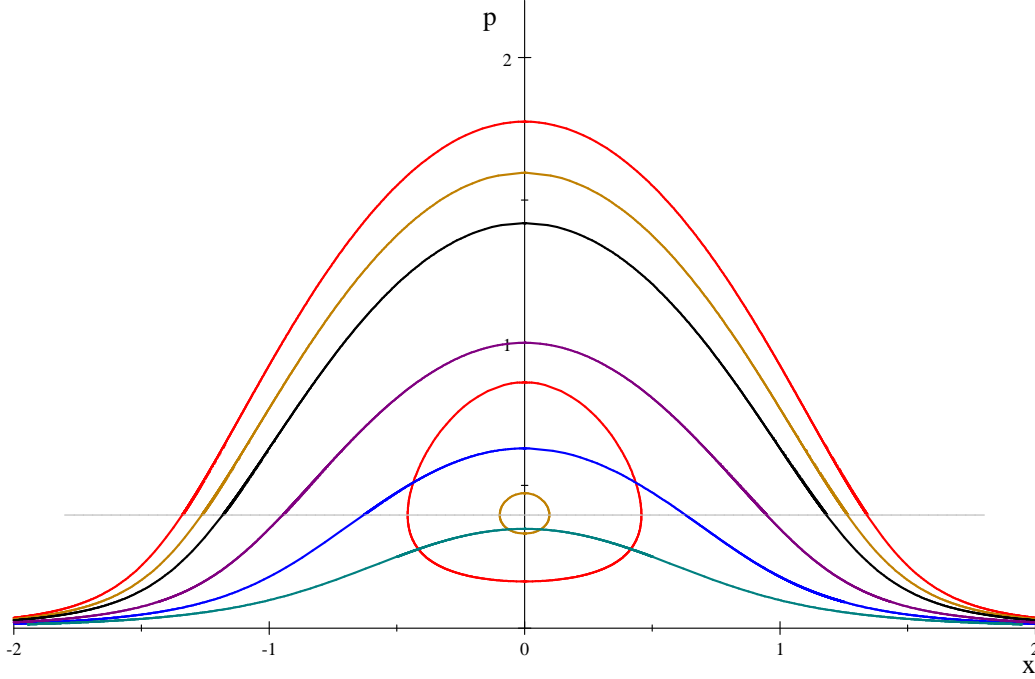
In fact, the $E < C$ classical situation provides intuition that is in accord with the features of the quantum ground state. For $E < C$, there are *no* classical trajectories (whether open and unbounded, or closed and bounded) in the $v < 1$ region governed by $H_+(x, p)$. For $E < C$, rather, there are only unbounded classical trajectories in the $v > 1$ region governed by $H_-(x, p)$. Hence, for $E < C$, a path integral of $\exp(iA/\hbar)$ would encounter no stationary points if restricted to trajectories in the $v < 1$ region. Moreover, there is an infinite, impenetrable E barrier separating classical solutions with $v < 1$ from those with $v > 1$, as is evident in the Figure below. This would suggest there are no admissible wave functions for $E < C$ with support in the region $v < 1$. Or, in terms of p , for energy less than C , there would be no admissible $\psi(p)$ energy eigenstates governed by H_+ . This heuristic argument is in agreement with the quantum features of the model.



$E(x, v)$ as given by (21) is clearly minimized on the (x, v) plane along the line $x = 0$, and less obviously for $v < 1$ at $v = 0$. This is evident in a graph of $E(x, v)|_{x=0}$ versus v . The minimum for $v < 1$ is at the (x, v) origin, where $E(0, 0) = C = \frac{3}{4^{2/3}} \approx 1.19$. The red dots on the E axis are the lowest two energy eigenvalues for the quantized model, namely, $E_0 = 0$ and $E_1 = 1.89379$.

Perhaps these classical features underpinning the quantized model become clearer upon considering trajectories as constant energy curves in (x, p) phase space. Several representative examples are shown in the next Figure (more details are available online). Two energies shown in the Figure allow both open, unbounded trajectories, and closed, bounded orbits, namely, for $E = 1.2$ and $E = 1.4$. As noted in the previous Figure, there is a critical energy, $E = C = \frac{3}{4^{2/3}} \approx 1.19$, below which bounded orbits do not occur.

When bounded orbits do exist, their turning points are given by $x = \pm\sqrt{E - C}$, corresponding to $v = 0$ in (21). However, at these turning points the momentum does *not* vanish, being given instead by $p = C/3 = \frac{1}{4^{2/3}} \approx 0.397$, as indicated by the horizontal light gray line in the Figure.



Supersymmetric model phase space trajectories are shown for various energies: $E = -0.5$ in blue-green, $E = 0$ in blue, $E = 0.5$ in purple, $E = 1$ in black, $E = 1.2$ in sienna, and $E = 1.4$ in red.

It is important to note in the Figure the counter-intuitive feature that $p > 0$ even when $v \leq 0$. Moreover, the phase space curves also exhibit quasi-Hamiltonian flow [6], as mentioned above for the gaussian model: Trajectories can cross each other on this (x, p) phase space plot. This is allowed when different Hamiltonian branches are governing the motion for the different curves that cross. That is to say, just like H , the trajectories are actually on two different branches of a phase space Riemann surface.

5 Deforming the supersymmetric Hamiltonians

Here we implement a deformation procedure [14, 15] to construct a family of related but modified Hamiltonians through the use of general solutions to the Riccati equation as obtained from particular solutions.

In addition to the square-integrable zero-energy solution of $H_- \psi = 0$, as given by

$$\left(\frac{d}{dp} + \sqrt{p} \right) \psi(p) = 0 \quad \text{i.e.} \quad \psi(p) = \exp\left(-2p^{3/2}/3\right), \quad (22)$$

the factorized Hamiltonian method may be used to construct another square-integrable solution, for a *modified* Hamiltonian, from the *non*-square-integrable zero-energy solution of $H_+ \phi = 0$, as given by

$$\left(\frac{d}{dp} - \sqrt{p} \right) \phi(p) = 0 \quad \text{i.e.} \quad \phi(p) = \exp\left(2p^{3/2}/3\right). \quad (23)$$

The construction involves the general solution of the Riccati equation $V_- = w^2 - w'$, as obtained from the particular one used above, $w_0(p) = \sqrt{p}$. This general solution involves the non-square-integrable ϕ ,

and a single constant of integration, κ . Thus

$$\begin{aligned} w_\kappa(p) &= w_0(p) - \frac{d}{dp} \ln \left(1 + \kappa \int_0^p e^{2 \int_0^s w_0(u) du} ds \right) \\ &= w_0(p) - \frac{\kappa e^{2 \int_0^p w_0(u) du}}{1 + \kappa \int_0^p e^{2 \int_0^s w_0(u) du} ds}. \end{aligned} \quad (24)$$

For the case at hand, this comes down to

$$w_\kappa(p) = \sqrt{p} - \frac{\kappa e^{4p^{3/2}/3}}{1 + \kappa g(p)} \quad (25)$$

$$= \sqrt{p} - \kappa e^{4p^{3/2}/3} + \kappa^2 e^{4p^{3/2}/3} g(p) + O(\kappa^3), \quad (26)$$

$$g(p) \equiv \int_0^p e^{4s^{3/2}/3} ds = p e^{\frac{4}{3} p^{\frac{3}{2}}} {}_1F_1 \left(1; 5/3; -\frac{4}{3} p^{\frac{3}{2}} \right). \quad (27)$$

So the subleading terms in this κ -deformation involve a confluent hypergeometric function (incomplete gamma). Note that $w_0(p) = w_\kappa(p)|_{\kappa=0}$. Also note that $w_\kappa^2 - w'_\kappa = p - \frac{1}{2\sqrt{p}}$ for any κ .

Now, a zero-energy eigenfunction of H_- constructed from the general w_κ is *not* square-integrable (except in the case $\kappa = 0$). However, a new square-integrable solution for a *modified* Hamiltonian $H_+(\kappa)$ can be constructed.

For any $\kappa > 0$ this solution is

$$\phi_0(p, \kappa) = \frac{\kappa e^{\int_0^p w_0(u) du}}{1 + \kappa \int_0^p e^{2 \int_0^s w_0(u) du} ds}, \quad (28)$$

where it is significant that the exponent in the numerator is one half that in w_κ . For the present case this is

$$\phi_0(p, \kappa) = \frac{\kappa e^{\frac{2}{3} p^{\frac{3}{2}}}}{1 + \kappa g(p)}. \quad (29)$$

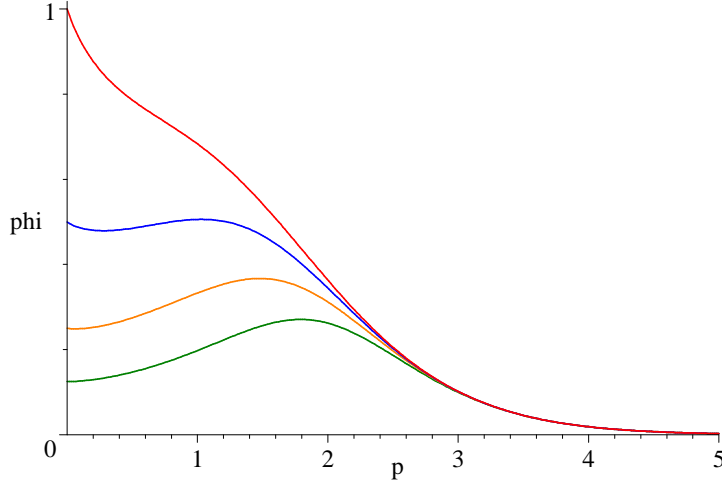
Note that this solution disappears in the undeformed limit, $\phi_0(p, \kappa)|_{\kappa=0} = 0$. Also note the square-integrability on the half-line, $0 \leq p \leq \infty$: This holds for the ϕ_0 wave functions, for all $\kappa > 0$. In the next Figure, we plot some representative $\phi_0(p, \kappa)$ for selected κ .

Boundary conditions. For general κ , ϕ_0 satisfies neither Neumann nor Dirichlet, but rather Robin boundary conditions³ depending on κ , namely,

$$\kappa \phi_0(0, \kappa) + d\phi_0(0, \kappa) / dp = 0. \quad (30)$$

This follows from $\phi_0(0, \kappa) = \kappa$, $d\phi_0(0, \kappa) / dp = -\kappa^2$.

³For example, see http://en.wikipedia.org/wiki/Robin_boundary_condition



$\phi_0(p, \kappa)$ for $\kappa = 1, 1/2, 1/4, \& 1/8$, in red, blue, orange, & green, respectively. Note that $\phi_0(p, 0) = 0$.

Of course, it is better to write the derivative of ϕ_0 at all values of $p \geq 0$ as a linear null equation:

$$\left(\frac{d}{dp} - w_\kappa(p) \right) \phi_0(p, \kappa) = 0. \quad (31)$$

In this form it is clear that $\phi_0(p, \kappa)$ is a square-integrable zero-energy solution of a κ -dependent class of Hamiltonians involving the general $w_\kappa(p)$:

$$\begin{aligned} H_+(\kappa) &= - \left(\frac{d}{dp} + w_\kappa(p) \right) \left(\frac{d}{dp} - w_\kappa(p) \right) \\ &= - \frac{d^2}{dp^2} + p + \frac{1}{2\sqrt{p}} - \frac{4\kappa\sqrt{p}e^{4p^{3/2}/3}}{1 + \kappa g(p)} + \frac{2\kappa^2 e^{8p^{3/2}/3}}{(1 + \kappa g(p))^2}. \end{aligned} \quad (32)$$

Note, then, that $H_+(\kappa)|_{\kappa=0} = H_+$, the initial undeformed Hamiltonian, as given in equation (13).

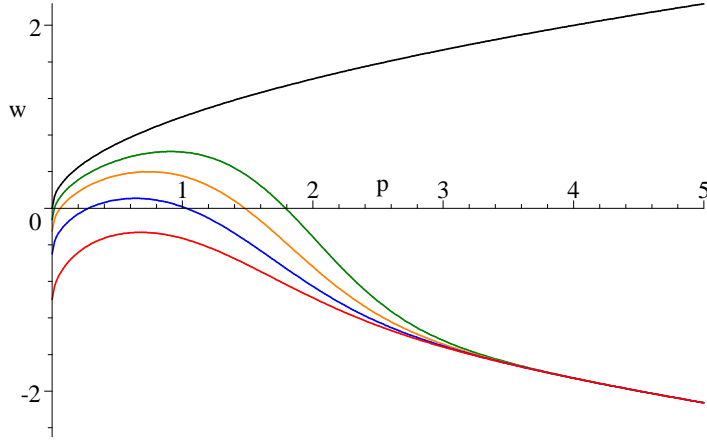
By way of comparison, $H_-(\kappa) = - \left(\frac{d}{dp} - w_\kappa(p) \right) \left(\frac{d}{dp} + w_\kappa(p) \right)$ does not participate in this deformation, as it is actually *independent* of κ , and identical to the previous H_- in equation (13). As mentioned earlier, in this case the κ -dependent zero energy eigenfunctions of H_- , as given by $\exp(-\int_0^p w_\kappa(s) ds)$, are *not* square-integrable except for $\kappa = 0$.

That is to say, the true ground state of H_- is indeed unique, and proportional to $\exp(-2p^{3/2}/3)$. The normalization of the true ground state is finite and given by $\int_0^\infty \exp(-4p^{3/2}/3) dp = \frac{1}{6^{1/3}} \Gamma(\frac{2}{3}) \approx 0.745$. On the other hand, it is informative to check that $\exp(-\int_0^p w_\kappa(s) ds)$ is *not* square integrable for $\kappa > 0$, where

$$w_\kappa(p) = \sqrt{p} - \frac{\kappa e^{4p^{3/2}/3}}{1 + \kappa g(p)}. \quad (33)$$

To see this, it is sufficient just to plot w_κ for a few values of κ and infer the general result.

For any $\kappa > 0$, it is evident from the Figure below that w_κ becomes negative and grows in magnitude for large enough p , asymptoting towards a common κ -independent function in the limit of large p . Thus we have $\int_0^p w_\kappa(u) du < 0$ for p sufficiently large, and hence $\int_0^\infty \exp(-2 \int_0^p w_\kappa(s) ds) dp$ will diverge.



$w_\kappa(p)$ for $\kappa = 1, 1/2, 1/4, \& 1/8$, in red, blue, orange, & green, respectively, along with $w_0(p) = \sqrt{p}$ in black.

The large p behavior of $w_\kappa(p)$ for $\kappa \neq 0$ may be seen analytically from the asymptotic behavior of (27), which gives

$$g(p) \underset{p \rightarrow \infty}{\sim} \frac{1}{2} \frac{e^{\frac{4}{3}p^{\frac{3}{2}}}}{\sqrt{p}} \left(1 + \frac{1}{2p^{\frac{3}{2}}} + O\left(\frac{1}{p^3}\right) \right), \quad w_\kappa(p) \underset{p \rightarrow \infty}{\sim} \sqrt{p} \left(-1 + \frac{1}{p^{\frac{3}{2}}} + O\left(\frac{1}{p^3}\right) \right). \quad (34)$$

As was the case for the undeformed model, there are some technical issues associated with probability flow and self-adjointness of the Hamiltonians when $\kappa \neq 0$. We are content to leave these issues as exercises for the interested reader.

6 Discussion

As emphasized by Shapere and Wilczek, “many worlds” systems with branched Hamiltonians are by no means rare, in theory. Here, we have displayed some simple unified Lagrangian prototype systems which, by virtue of non-convexity in their velocity dependence, branch into double-valued (but still self-adjoint) Hamiltonians.

We have outlined a gaussian model whose branches lie on a compact, closed momentum manifold with coalescing cusps at finite p , as a preliminary step in the search for a supersymmetric model with similar properties. We then discussed a class of models with double-valued Hamiltons, one of which has the canonical structure of a supersymmetric pair of Hamiltonians. We have surveyed the spectral and boundary condition linkages involved across the respective branches for this supersymmetric model, in a uniform framework, by utilizing the eigenstate-linking supercharge ladder operators (but which are *not* Grassmann and which do *not* commute with the two Hamiltonians).

These particular branched Hamiltonians — although living in “two worlds” — are nevertheless paired by supercharges into a uniform Darboux isospectral system, in the very same Hilbert space; and yet they are inexorably separated, in some analogy to fermionic and bosonic sectors, as the respective dynamical intervals only connect at $p = \infty$. In this respect, this particular supersymmetric system differs from more typical constructions given by Shapere and Wilczek, which exhibit similar operator branching structures but connect for finite p .

Acknowledgements: *This work was supported in part by NSF Award PHY-1214521; and in part, the submitted manuscript has been created by UChicago Argonne, LLC, Operator of Argonne National Laboratory. Argonne, a U.S. Department of Energy Office of Science laboratory, is operated under Contract No. DE-AC02-06CH11357. The U.S. Government retains for itself, and others acting on its behalf, a paid-up nonexclusive, irrevocable worldwide license in said article to reproduce, prepare derivative works, distribute copies to the public, and perform publicly and display publicly, by or on behalf of the Government. TLC was also supported in part by a University of Miami Cooper Fellowship.*

References

- [1] A Shapere and F Wilczek, “Branched Quantization” *Phys.Rev.Lett.* 109 (2012) 200402 (e-Print: arXiv:1207.2677 [quant-ph]) DOI: 10.1103/PhysRevLett.109.200402
- [2] A Shapere and F Wilczek, “Classical Time Crystals” *Phys.Rev.Lett.* 109 (2012) 160402 (e-Print: arXiv:1202.2537 [cond-mat.other]) DOI: 10.1103/PhysRevLett.109.160402
- [3] A D Shapere, F Wilczek, Z Xiong, “Models of Topology Change” (e-Print: arXiv:1210.3545 [hep-th])
- [4] F Wilczek “Quantum Time Crystals” *Phys.Rev.Lett.* 109 (2012) 160401 (e-Print: arXiv:1202.2539 [quant-ph]) DOI: 10.1103/PhysRevLett.109.160401
- [5] T L Curtright and C K Zachos, “Evolution profiles and functional equations” *J.Phys.* A42 (2009) 485208 (eprint: arXiv:0909.2424 [math-ph]) DOI: 10.1088/1751-8113/42/48/485208
- [6] T L Curtright and C K Zachos, “Chaotic Maps, Hamiltonian Flows, and Holographic Methods” *J.Phys.* A43 (2010) 445101 (e-Print: arXiv:1002.0104 [nlin.CD]) DOI: 10.1088/1751-8113/43/44/445101
- [7] T L Curtright and A Veitia, “Logistic Map Potentials” *Phys.Lett.* A375 (2011) 276-282 (eprint: arXiv:1005.5030 [math-ph]) DOI: 10.1016/j.physleta.2010.11.019
- [8] T L Curtright, “Potentials Unbounded Below” *SIGMA* 7 (2011) 042 (eprint: arXiv:1011.6056 [math-ph]) DOI: 10.3842/SIGMA.2011.042
- [9] T L Curtright and C K Zachos, “Renormalization Group Functional Equations” *Phys.Rev.* D83 (2011) 065019 (e-Print: arXiv:1010.5174 [hep-th]) DOI: 10.1103/PhysRevD.83.065019
- [10] T L Curtright, X Jin, and C K Zachos “RG flows, cycles, and c-theorem folklore” *Phys.Rev.Lett.* 108 (2012) 131601 (e-Print: arXiv:1111.2649 [hep-th]) DOI: 10.1103/PhysRevLett.108.131601
- [11] E Witten, “Supersymmetry and Morse Theory” *J.Diff.Geom.* 17 (1982) 661-692; “Constraints on Supersymmetry Breaking” *Nucl.Phys.* B202 (1982) 253-316 DOI: 10.1016/0550-3213(82)90071-2
- [12] R Shankar, “Solvable Models With Selftriality in Statistical Mechanics and Field Theory” *Phys.Rev.Lett.* 46 (1981) 379 DOI: 10.1103/PhysRevLett.46.379
- [13] E P Wigner, “Die Messung quantenmechanischer Operatoren” *Z. Phys.* 133 (1952) 101-108 DOI: 10.1007/BF01948686; G C Wick, A S Wightman, and E P Wigner, “The Intrinsic Parity of Elementary Particles” *Phys.Rev.* 88 (1952) 101-105 DOI: 10.1103/PhysRev.88.101, and “Superselection Rule for Charge” *Phys.Rev.* D 1 (1970) 3267-3269 DOI: 10.1103/PhysRevD.1.3267
- [14] B Mielnik, “Factorization method and new potentials with the oscillator spectrum” *J.Math.Phys.* 25 (1984) 3387-3389 DOI: 10.1063/1.526108
- [15] J O Rosas-Ortiz, “On the factorization method in quantum mechanics” *Proceedings of the First International Workshop on “Symmetries in Quantum Mechanics and Quantum Optics”* A. Ballesteros et al (Eds.), Servicio de Publicaciones de la Universidad de Burgos (Spain), p. 285-299. Burgos, Spain (1999) (e-Print: arXiv:quant-ph/9812003)